Eur Biophys J (2004) 33: 159–166
DOI 10.1007/s00249-003-0351-6

ARTICLE

J. A. Tuszyński · E. J. Carpenter · J. M. Dixon
Y. Engelborghs

Non-Gaussian statistics of the vibrational fluctuations of myoglobin

Received: 3 January 2003 / Revised: 19 July 2003 / Accepted: 19 July 2003 / Published online: 19 September 2003

Abstract Experiments on the dynamics of vibrational fluctuations in myoglobin revealed an interesting behavioral cross-over occurring in the range 180–200 K. In this temperature range the mean square displacement of atomic positions versus temperature sharply increases its slope, indicating the dissociation of CO from the heme group. In this paper we develop a theoretical model that provides a framework for the quantitative description of this phenomenon. The basis of our calculations is an assumption of an effective potential with multiple local minima. In particular, we consider a quartic potential in place of the simple quadratic. We then use non-Gaussian statistics to obtain a relationship between the mean square displacement and model parameters. We compare our model to published experimental data and show that it can describe the data set using physically meaningful parameters which are fitted to the experimental data. In the process we verify the Gaussian approximation's applicability only to the low-temperature régime. In the high-temperature limit, however, deviations from the Gaussian approximation are due to the double-well nature of our effective potential. We find that the published datasets showing the thermal transition display the qualitative trends predicted by appropriate algebraic approximations to our predicted myoglobin behavior.

J. A. Tuszyński (✉) · E. J. Carpenter
Department of Physics, University of Alberta,
Edmonton, Alberta, T6G 2J1, Canada
E-mail: jtus@phys.ualberta.ca
Fax: +1-780-4920714

J. M. Dixon
Department of Physics, University of Warwick,
Coventry, CV4 7AL, UK

Y. Engelborghs
Laboratory of Biomolecular Dynamics, University of Leuven,
Celestijnenlaan 200D, B-3001 Leuven, Belgium

Keywords Conformational changes · Myoglobin · Non-Gaussian statistics · Protein dynamics · Thermal fluctuations

Introduction

Protein structure and function determination is one of the central problems of modern biophysics and biochemistry (Branden and Tooze 1999). Among the million or so proteins identified by cell biologists, a special place is held by functional proteins such as motor proteins or enzymes (Berg et al. 2002). Despite the many advances in our understanding of how proteins fold and function, molecular level insights into these mechanisms often remain elusive. Proteins exhibit dynamic complexity with different regions, referred to as functional domains, of the same protein often showing different types of activity. Of special importance to the biological functioning of proteins are structure fluctuations that are induced by binding to ligands or substrates. Such is the case of myoglobin, where the oxygen ligand has to diffuse through the protein matrix before it is able to bind to the iron in the heme group (Frauenfelder et al. 1998).

Owing to a wide range of characteristic time scales, from picoseconds to tens of seconds, experimental studies are fraught with difficulties. One of the best characterized functional proteins is myoglobin, the dynamics of which have been experimentally studied using inelastic scattering of synchrotron radiation (Parak and Achterhold 1999), phonon assisted Mössbauer scattering (Achterhold et al. 2002), time resolved spectroscopy (Ostermann et al. 2000), and Mössbauer absorption spectroscopy (Parak et al. 1982; Neinhaus et al. 2001; Parak 2001), in addition to standard X-ray crystallography (Nienhaus et al. 1989). In this paper we analyze some of the experimental results for myoglobin using non-Gaussian statistical methods (Tuszyński et al. 1985; Tuszyński and Wierzbicki 1991) applied to the

temperature dependence of the positional fluctuations. The objective of the present study is to provide a powerful theoretical tool in the analysis of the conformational changes that are essential for protein molecules in order that they may carry out their functions.

Non-Gaussian analysis of conformational dynamics

Myoglobin is a protein (see Fig. 1 for an illustration of its structure) consisting of 153 amino acids and one heme group of protoporphyrin IX with an iron atom in the centre (Parak and Achterhold 1999). The molecular weight of myoglobin is approximately 17.8 kDa. The three-dimensional folding of myoglobin produces a globular structure with a diameter of about 3 nm. Myoglobin's function is to store oxygen provided by the blood until it is released for some form of metabolic activity. The molecular oxygen binds at the active site of the protein and one of the six coordinations of the iron atom. The remaining five are taken up by four nitrogen atoms and one bond to the protein matrix. The process of binding and releasing of the ligand is reversible (Parak and Achterhold 1999; Ostermann et al. 2000).

Recent experiments using Mössbauer absorption (Achterhold at al. 2002), as well as several other experimental methods (Parak and Achterhold 1999; Ostermann et al. 2000), provided insights into the kinetics and dynamics of myoglobin's conformational changes. In particular, flash photolysis was used to obtain an effective potential in terms of a reaction coordinate (Ostermann et al. 2000). It shows a global minimum at a bound state A and two local minima states at photoproduct states B_2 and B_3 whose activation energies have been estimated as 6.1 kJ/mol between B_2 and A, 11.1 kJ/mol between B_2 and B_3, and 22.4 kJ/mol between B_3 and B_2. This qualitatively indicates a three-well effective potential structure that underlies the protein conformational dynamics.

Parak and Achterhold (1999) used inelastic Rayleigh scattering of Mössbauer radiation to determine the temperature dependence of the mean square displacement, $<x^2>$, in myoglobin. It is interesting to note that in the low-temperature range from 0 K to approximately 180 K the dependence on temperature is linear, and given by $<x^2>/T = 2.1\times10^{-4}$ Å^2/K for the average position of atoms in the protein from linear regression, while the slope of $<x^2>/T = 0.6\times10^{-4}$ Å^2/K was obtained for the iron atom in deoxymyoglobin (Mbdeoxy) crystals. In the high-temperature régime, between 180 K and 300 K, the slope of these curves increases dramatically, by a factor of more than 10 in one case. The authors attribute the low-temperature behavior to harmonic motions of the protein, with the high-temperature behavior indicative of diffusive motion limited by the bonding forces within the protein.

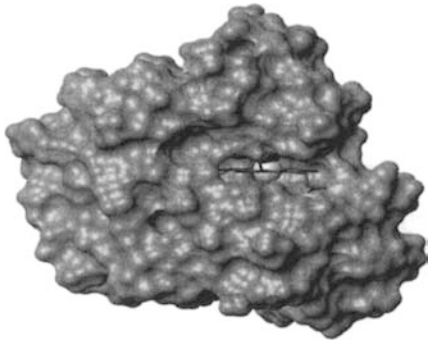

Fig. 1 Three-dimensional structure of myoglobin

In parallel to the experimental studies, a formidable computational effort was undertaken to evaluate myoglobin's dynamics using molecular dynamics simulations (Steinbach and Brooks 1993, 1996). Interestingly, a very similar qualitative picture of the mean square fluctuations as a function of temperature emerged. The effect depends on the level of hydration, with the extreme of dry samples (Ferrand et al. 1993), or suitably coated ones (Cordone et al. 1999), remaining harmonic at or above room temperature. In the remainder of this paper we will attempt to present a relatively simple explanation that is consistent with the model of thermal fluctuations in a system with multiple potential minima corresponding to the protein's stable conformations. This is in agreement with the results of conformational kinetics obtained by Ostermann et al. (2000). To make a direct comparison, we will additionally use the experimental data points for the iron atom's positional fluctuations measured by Mössbauer absorption as well as results for independent molecular dynamics simulations performed for myoglobin.

The model and its results

Parak and Achterhold (1999) reported two sets of data involving the temperature dependence of the mean square displacement, $<x^2>$, in myoglobin. The first set refers to the protein as a whole and the second only to the iron atom in Mbdeoxy crystals. Both plots (see their Figs. 6 and 7) exhibit a cross-over from a linear $<x^2>$ versus T dependence at low temperatures to a more rapidly increasing function at high temperatures. A double-well potential has been used by Doster et al. (1989) to explain elastic incoherent neutron scattering data on myoglobin. It is evident from the fits produced by Parak and Achterhold, on the basis of normal-mode analysis, that this approach fails to capture the cross-over and deviates in the high-temperature régime, producing a rapidly increasing error as the temperature increases. In this paper we attempt to develop a self-consistent model for both experiments and both thermal régimes.

In order to provide a simple model of fluctuational dynamics in the myoglobin matrix, we postulate an effective potential of the form (see Fig. 2):

$$V(x) = ax^4 + bx^3 + cx^2 + V_0 \tag{1}$$

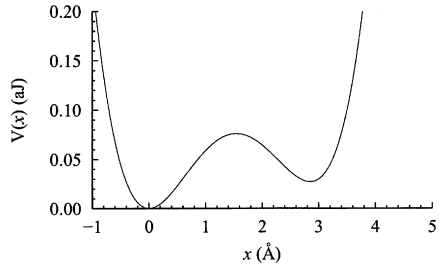

Fig. 2 An effective potential illustrating Eq. (1)

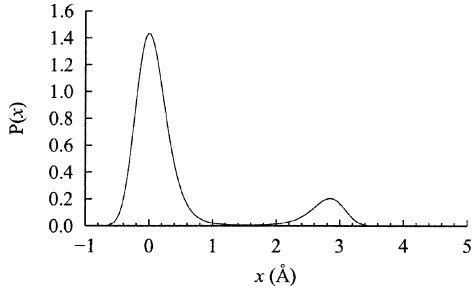

Fig. 3 The probability distribution $P(x)$ corresponding to Fig. 2

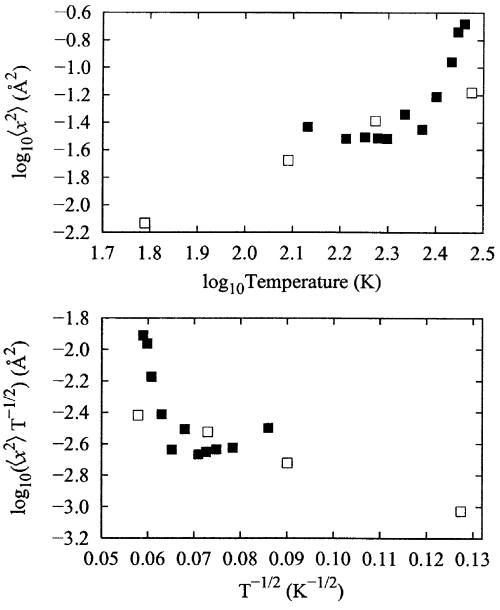

Fig. 4 Temperature dependence of the mean square displacement, $<x^2>$, over all atoms in myoglobin, measured by inelasic Rayleigh scattering. Radiation from ^{57}CoCr Mössbauer source (*filled squares*) and sychrotron (*open squares*). Plotted as (*top*) log–log with best-fit by the line $\log<x^2> = 1.28\log(T) - 4.35$ and (*bottom*) log–inverse square root with best-fit by the line $\log(<x^2>/\sqrt{T}) = -176/\sqrt{T} + 5.82$. Data source: Fig. 6 in Parak and Achterhold (1999)

which accounts for the bistability of the potential under certain assumptions about the coefficients. We selected this form using Fig. 4c from Ostermann et al. (2000) as a guide. We are ignoring the intermediate region at B_2 due to the small potential barrier between B_2 and A and the fact that if we were to include it, we would be forced to introduce additional adjustable parameters. The variable x in Eq. (1) is a spatial coordinate that we map to the reaction coordinate shown in the original figure.

We intend to develop a statistical approach for the calculation of average fluctuations over the entire range of temperatures. The conceptual reasoning involved is the Boltzmann probability distribution $P(x)$ given by:

$$P(x) = Z^{-1}\mathrm{e}^{-\beta V(x)} \tag{2}$$

where the normalizing factor is the corresponding partition function given by:

$$Z = \int_{-\infty}^{\infty} \mathrm{e}^{-\beta V(x)}\mathrm{d}x \tag{3}$$

This Boltzmann averaging technique leads to:

$$<x^2> = \int x^2 \frac{\mathrm{e}}{\int \mathrm{e}^{-\beta V(x)}\mathrm{d}x} \tag{4}$$

for the positional variance, $<x^2>$, measured about the origin, where the integrations are over all space. Unfortunately, our experimentally guided model requires the use of an anharmonic potential, so these integrals are non-Gaussian and the solutions are not simple. We note that the experimental data we use are of fluctuations about a mean position, which is not exactly the same as our choice of about the potential minimum; this difference will change $<x^2>$ by the square of the mean position, which is zero for harmonic wells. We estimate the size of this difference later. Also note that the constant term, V_0, in the potential becomes the multiplicative constant $\mathrm{e}^{-\beta V_0}$ in Eqs. (2, 3, 4) and therefore does not affect the distribution.

It is convenient to introduce parameters which can be directly linked to the experimental data. The first is the depths of the potential energy wells, which we denote by d_A and d_B, where the A and B refer to the deep and shallow wells, respectively.

A third parameter which controls the width of the lowest energy well we call w. At low temperatures the fluctuational motion is limited to within the confines of the dominant probability peak of $P(x)$ (see Fig. 3). Above some transition temperature, T_t, the molecule begins to explore the vicinity of the second equilibrium conformation, as manifested by the smaller probability peak. In this régime the Taylor expansion of $V(x)$ about its lowest minimum, x_A, is:

$$V(x) = \sum_{i=0}^{\infty}\left(\frac{1}{i!}\left(\frac{\mathrm{d}}{\mathrm{d}x^i}\right)_{x_A}(x - x_A\right)^i\Bigg) \tag{5}$$

and is dominated by the parabolic term in the expansion near the minimum (the linear coefficient is zero at the minimum). For a pure harmonic (parabolic) potential, $V(x) = V_0 + w_0x^2$, the mean square displacement is linear

with temperature and is just $<x^2> = (k_B T)/(2w_0)$. Using $(<x^2>/T)_{T<T_t}$ for the low-temperature slope, we therefore require that:

$$w = \frac{k_B}{2(<x^2>/T)_{T<T_t}} \tag{6}$$

and:

$$w = \frac{1}{2}\left(\frac{d^2V}{dx^2}\right)_{x_A} \tag{7}$$

Appendix A provides a description of how any given choice of the three physical constants d_A, d_B, and $(<x^2>/T)_{T<T_t}$ gives a unique potential by fixing the three coefficients a, b, and c.

We can now proceed to estimate the temperature dependence of the actual mean square displacement over the entire temperature régime.

The method

To calculate the mean square displacement at a temperature, T, we use Boltzmann statistics so that:

$$<x^2> = I_2/I_0 \tag{8}$$

where:

$$I_k = \int_{-\infty}^{\infty} x^k e^{-\beta(ax^4+bx^3+cx^2+V_0)} dx \tag{9}$$

In order to obtain a rapidly convergent series approximation for I_k we expand the cubic term in the exponential, bearing in mind that the quartic term will be dominant. Thus:

$$I_k = e^{-\beta V_0} \int_{-\infty}^{\infty} x^k e^{-\beta(ax^4+cx^2)} \left\{1 - \beta b x^3 + \frac{\beta^2 b^2 x^6}{2!} - \frac{\beta^3 b^3 x^9}{3!} + \ldots\right\} dx \tag{10}$$

Each of the integrals in Eq. (10) can be evaluated analytically in terms of parabolic cylinder functions (see Appendix B). Using the procedure described in Appendix B we find that in the high-temperature limit for which x is small we obtain:

$$<x^2> \approx 0.478 \frac{1}{\sqrt{2\beta a}} e^{-\beta c/\sqrt{2\beta a}} \left\{1 + \frac{\beta^2 b^2}{2!} \frac{1}{(2\beta a)^{3/2}} 2^{-3/2} \left[-2.028 e^{-\sqrt{3}\beta c/\sqrt{2\beta a}} + 7.397 e^{-\beta c/\sqrt{2\beta a}}\right] \ldots\right\} \tag{11}$$

In the opposite régime, for low temperatures, with $x >> 1$, we find that:

$$<x^2> \approx \frac{1}{2\beta c}\left\{1 + \frac{45}{b^2}\beta c^3 \ldots\right\} \tag{12}$$

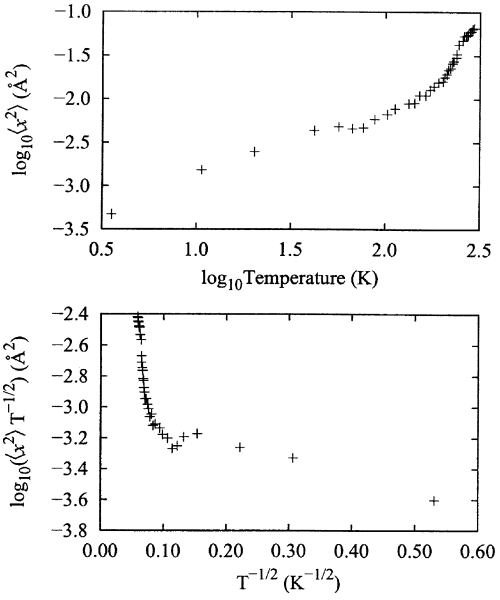

Fig. 5 Temperature dependence of $<x^2>$ for the iron atom in Mbdeoxy crystals. Plotted as (*top*) log–log and (*bottom*) log–inverse square root. Data source: Fig. 7 in Parak and Achterhold (1999)

where in both equations Eqs. (11) and (12) we have retained two terms in I_2 and I_0 from Eqs. (B2) and (B3) and used the limits in Eqs. (B4) and (B5).

We can therefore conclude that spatial fluctuations in an anharmonic potential should manifest themselves by a predominantly linear temperature dependence with small power law corrections, provided the temperature is low enough. In the high-temperature régime, however, positional fluctuations are dominated by the product of an exponential decay with an inverse square root dependence on temperature and a square root of temperature pre-factor. Corrections to this behavior are approximately similar to the leading term but without the pre-factor.

In order to support the results of our calculations, we have replotted the data sets from Parak and Achterhold (1999) for the average atomic coordinates and for the iron atom using two different coordinate representations. First, plotting the data with a log–log scale we show a linear dependence of the first half of the curve $<x^2>$ versus T for $T < T_t$. The high-temperature range, $T > T_t$, in both cases follows a modified exponential dependence and thus we have also plotted $\ln(<x^2>/\sqrt{T})$ versus $1/\sqrt{T}$. It is clear from these two data sets (see Figs. 4 and 5) (Parak and Achterhold 1999) that the low-temperature data points follow a linear trend with temperature while the high-temperature data points are best described by a function

proportional to $\sqrt{T}\exp(-\lambda/\sqrt{T})$. Furthermore, we have similarly re-analysed data from the molecular dynamics simulations of hydrated and dehydrated carboxymyoglobin (MbCO) published originally by Steinbach and Brooks (1993, 1996). Again, the same qualitative trend prevails, showing a cross-over from a linear to a modified exponential dependence on temperature in myoglobin's vibrational fluctuations. Figures 6, 7, 8, 9, 10

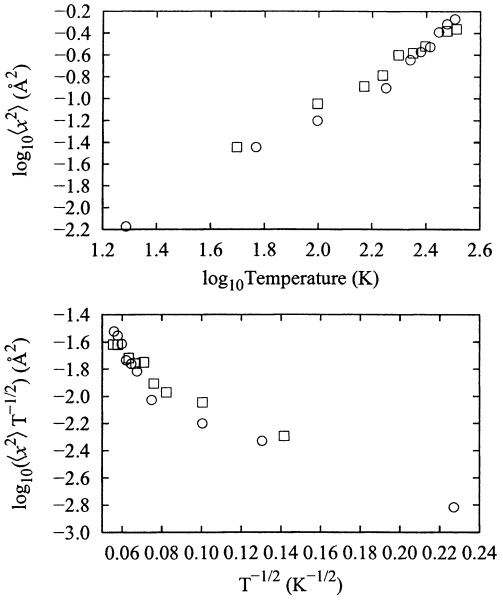

Fig. 6 Temperature dependence of $< x^2 >$ for MbCO hydrated with 0 (*boxes*) and 350 (*circles*) water molecules. Plotted as (*top*) log–log and (*bottom*) log–inverse square root. Data source: Fig. 3A in Steinbach and Brooks (1993)

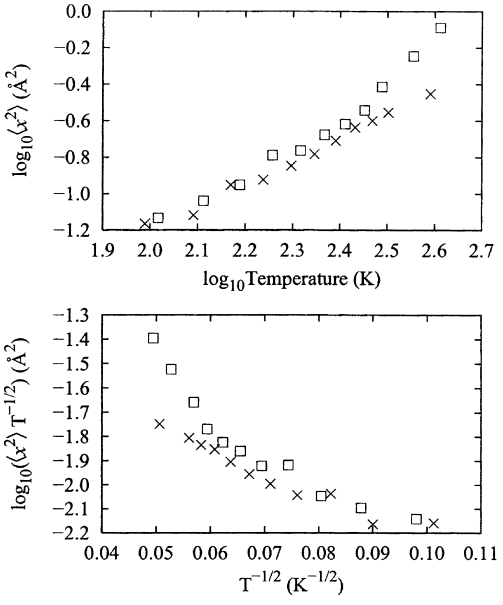

Fig. 7 Temperature dependence of $< x^2 >$ for dehydrated (0 water molecules) MbCO averaged over all atoms with dihedral transitions (*boxes*) and without (*crosses*). Plotted as (*top*) log–log and (*bottom*) log–inverse square root. Data source: Fig. 2A in Steinbach and Brooks (1996)

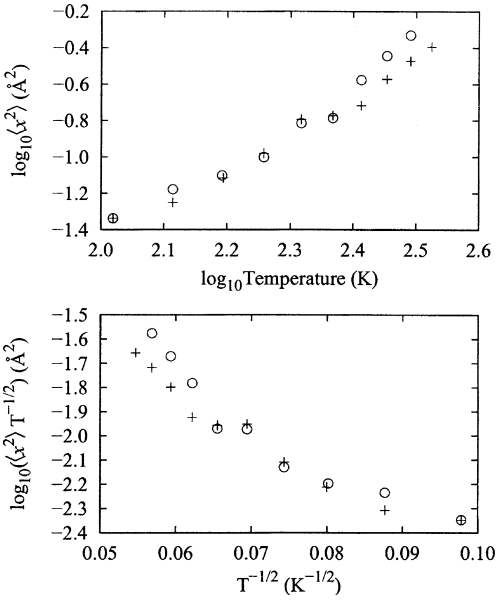

Fig. 8 Temperature dependence of $< x^2 >$ for hydrated (350 water molecules) MbCO averaged over all atoms with dihedral transitions (*circles*) and without (*pluses*). Plotted as (*top*) log–log and (*bottom*) log–inverse square root. Data source: Fig. 2B in Steinbach and Brooks (1996)

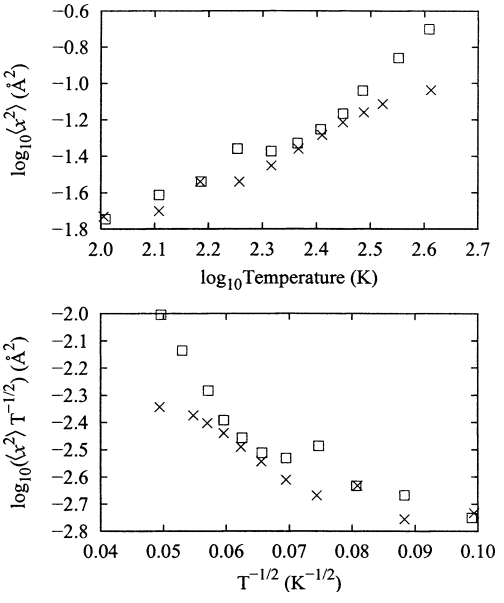

Fig. 9 As in Fig. 7, but plotting the mass weighted variance in position, $< x^2 >$, over the eight α-helix centres of mass. Data source: Fig. 3A in Steinbach and Brooks (1996)

summarise the data of Steinbach and Brooks (1993, 1996) appropriately replotted. The first set of figures describes the data sets of Parak and Achterhold for $< x^2 >$ versus T as an average of all atoms in metmyoglobin crystals and the iron atoms in Mbdeoxy crystals. This set is followed by the data for dehydrated and hydrated MbCO (Steinbach and Brooks 1996) and finally the molecular dynamics simulations (Steinbach and

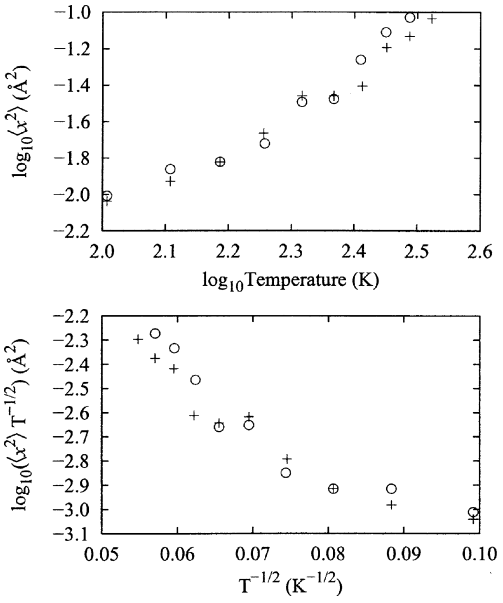

Fig. 10 As in Fig. 8, but plotting the mass weighted variance in position, $<x^2>$, over the eight α-helix centres of mass. Data source: Fig. 3B in Steinbach and Brooks (1996)

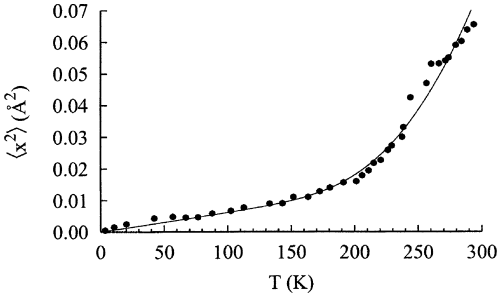

Fig. 11 Temperature dependence of $<x^2>$ for Eq. (1) using the parameters in Eq. (13) (*solid line*) and as in Fig. 7 in Parak and Achterhold (1999) (*dots*)

Brooks 1993) for hydrated MbCO. All these data sets fully support our model predictions in terms of the trend in the $<x^2>$ versus T dependence.

It is worth emphasising that the above calculation is quite general and applies to any anharmonic potential, including situations with two local minima separated by a potential barrier. The key message of these calculations is that a cross-over occurs in the temperature dependence of $<x^2>$ from a linear function of T to one which is dominated by an exponential dependence. We have supported this prediction with a number of data sets for myoglobin originating from the work of other authors. What this means physically is that, at temperatures below the cross-over temperature of ~200 K, spatial fluctuations are dominated by oscillations in the harmonic potential around the ground state. Once the cross-over temperature is reached, the molecule is allowed to explore higher energy states, including the vicinity of the second local minimum (see Fig. 2).

The actual shape of this effective potential may be more complicated than the postulated form of Eq. (1). However, the qualitative features should remain the same. Furthermore, the effective potential depends on the type of myoglobin, the degree of hydration and solvation of the molecule, as well as whether the average is taken over all atoms or just the iron atom. As an illustration, we have selected the data set from Fig. 7 of Parak and Achterhold (1999) and made a fairly accurate fit to the thermal fluctuation data using a quartic polynomial function for the effective potential as described above. We set the low-temperature slope to the value 0.6×10^{-4} Å^2/K that the authors reported in the text and choose $d_B = 22.4$ kJ/mol as reported in Fig. 4c from Ostermann et al. (2000). We can then plot $<x^2>$ versus T using Eq. (4). We find the choice of $d_A = 4150$ K $= 34.5$ kJ/mol results in the curve shown in Fig. 11.

Note that the heights of the potential barriers are of the same order of magnitude as typical hydrogen bond energies. This is consistent with the role of thermal fluctuations in bond-breaking leading to a conformational change. The resulting effective potential coefficients are:

$$\begin{aligned} a &= +1.52 \times 10^{-20}\ \text{J/Å}^4 \\ b &= +4.33 \times 10^{-21}\ \text{J/Å}^3 \\ c &= -5.29 \times 10^{-20}\ \text{J/Å}^2 \end{aligned} \tag{13}$$

It can be immediately seen from the diagram that the quantitative agreement with the data is very good; the differences in our fit value of $<x^2>$ resulting from the choice of a fixed origin rather than the thermally variable mean are less than 4% in the curve of Fig. 11. Notably, the deviations below 200 K are less than 1%.

Finally, we wish to comment about the calculations presented in a recent paper (Achterhold et al. 2002) using the vibrational mode energy ε and the density of states $D(\varepsilon)$ through the formula:

$$<x^2(T,\varepsilon)> = \frac{\hbar^2}{m_{\text{Fe}}} \int_0^{\varepsilon} \frac{D(\tilde{\varepsilon})}{\tilde{\varepsilon}} \left(\frac{1}{e^{\tilde{\varepsilon}/k_B T} - 1} + \frac{1}{2} \right) d\tilde{\varepsilon} \tag{14}$$

This leads to good agreement at low temperatures but is very poor at high temperatures. Above 200 K the above formula predicts a continuation of the linear trend, but with small corrections. Clearly, since this is based on a harmonic approximation, there is no possibility of obtaining behavior consistent with the experimental data unless the anharmonicity of the system is accounted for. We believe that myoglobin is no exception here and similar conclusions can be expected for all proteins which undergo significant conformational changes. A recent paper (Tama et al. 2000) analysed molecular dynamics simulations of human lysozyme and concluded that the large volume fluctuations observed in the simulations require the inclusion of anharmonic

potential terms and consequently non-Gaussian fluctuations. We could not agree more. Moreover, we foresee the usefulness of our non-Gaussian approach in the description of virtually all functional proteins. A case in point is the motor domain of kinesin that changes conformation depending on whether ATP or ADP molecules are bound to it. Since activation of the processivity of kinesin's motion is temperature dependent (Howard 2001), this effect is also expected to strongly involve non-Gaussian fluctuations. Clearly this connection between a protein's structural bistability and the statistics of thermal fluctuations offers a key insight into the activation of biological functions.

Summary

This paper has been concerned with the behavior of the positional thermal fluctuations of myoglobin over a large temperature range, from 0 K to 300 K. The data that we analysed came from both experiments on and molecular dynamics simulations of myoglobin. The experiments on the vibrational dynamics of myoglobin used a variety of techniques, including the phonon-assisted Mössbauer effect, Mössbauer absorption spectroscopy, and inelastic scattering of synchrotron radiation. Several variants of myoglobin were investigated and the molecular dynamics simulations of MbCO involved several levels of hydration. All these data sets, however, had one thing in common, namely a pronounced signature of anharmonic fluctuations above a threshold temperature of ~200 K. Until now, modeling efforts have stopped short of accounting for anharmonicity using non-Gaussian statistics and this therefore was the objective of our paper. We have provided a relatively simple effective potential that accounts for the two local minima corresponding to the two conformational states of the protein, separated by a potential barrier. The height of the potential difference determines the value of the cross-over temperature. The curvature of the potential around the ground state minimum that defines the slope is the $<x^2>$ versus T line at low temperatures. Finally, anharmonicity in the form of a quartic term produces good qualitative agreement with all the data sets analysed. We have also found a very reasonable quantitative fit to one particular case which was selected (it had the most data points) to provide an example. We believe the method presented here is sufficiently general to be applicable to the analysis of conformational effects in proteins. While molecular dynamics simulations can provide an accurate tool in the quantification of the conformational energy landscape, the non-Gaussian statistical analysis described in this paper can be used in the prediction of functional transitions that are triggered by thermal fluctuations.

Acknowledgements This research has been supported by MITACS, NSERC, and the Theoretical Physics Institute of the University of Alberta. Part of this research was carried out with the support of a senior fellowship for J.A.T. at the University of Leuven. We wish to thank Mr. W. Malinski for his assistance in data analysis. J.M.D. would like to thank the staff and members of the Physics Department, University of Alberta, for all their kindness and thoughtfulness during his stay.

Appendix

Appendix A: derivation of potential

In this appendix we show how to fix the three parameters a, b, and c to provide a unique potential. We consider Eqs. (1), (6), $V(x_A) = d_A$ (by definition), and choose $x_A < x_B$; it is then possible to obtain by algebraic manipulation:

$$a = \frac{c^2 - w^2}{12 d_A} \tag{A1}$$

$$b = \sqrt{\frac{2(c-w)(2c+w)^2}{27 d_A}} \tag{A2}$$

Further algebra and the change of variable $c = fw$ produces:

$$r = \frac{d_B}{d_A} = \frac{f^3(f+2)}{(f-1)(f+1)^3} \tag{A3}$$

We are interested in the case that $0 \geq r \geq 1$, $r \in \mathbf{R}$. It can be shown that while in general there are four roots for f, only one:

$$f = -\left(\frac{1}{2}\right) + \frac{1}{2}\sqrt{1 + \frac{2^{2/3} r^{1/3}}{(r-1)^{2/3}}} - \frac{1}{2}\sqrt{2 - \frac{2^{2/3} r^{1/3}}{(r-1)^{2/3}} + \frac{-8 + \frac{16r}{r-1}}{4\sqrt{1 + \frac{2^{2/3} r^{1/3}}{(r-1)^{2/3}}}}} \tag{A4}$$

corresponds to the case we are interested in and lies in the range $[0, -1/2]$.

Appendix B: derivation of $<x^2>$

Each of the integrals in Eq. (10) can be evaluated using the formula (Tuszyński et al. 1985, 1986; Tuszyński and Wierzbicki 1991):

$$\int_0^\infty y^{2mp-1} \mathrm{e}^{-By^{2m} - Fy^{4m}} \mathrm{d}y = (2m)^{-1} (2F)^{-p/2} \Gamma(p) D_{-p}\left(B(2F)^{-1/2}\right) \mathrm{e}^{B^2/2F} \tag{B1}$$

where D_{-p} is a parabolic cylinder function and $\Gamma(p)$ a standard Gamma function (Abramowitz and Stegun 1972). Applying this method we obtain:

$$I_2 = \mathrm{e}^{-\beta V_0}\mathrm{e}^{\beta^2 c^2/2\beta a}\sum_{q=0}^{\infty}\frac{1}{(2\beta a)^{\frac{3+6q}{4}}}\Gamma\left(\frac{3+6q}{2}\right)D_{-\frac{3+6q}{2}\frac{\beta c}{\sqrt{2\beta a}}}\frac{(\beta b)^{2q}}{(2q)!} \tag{B2}$$

and:

$$I_0 = \mathrm{e}^{-\beta V_0}\mathrm{e}^{\beta^2 c^2/2\beta a}\sum_{q=0}^{\infty}\frac{1}{(2\beta a)^{\frac{1+6q}{4}}}\Gamma\left(\frac{1+6q}{2}\right)D_{-\frac{1+6q}{2}}\frac{\beta c}{\sqrt{2\beta a}}\frac{(\beta b)^{2q}}{(2q)!} \tag{B3}$$

The parabolic cylinder function has two well-known asymptotic limits, namely for $x \approx 0$:

$$D_{-a-12}(\pm x) \approx \mathrm{e}^{\mp\sqrt{ax}}\left[\frac{\sqrt{\pi}2^{-\frac{a}{2}-\frac{1}{4}}}{\Gamma\left(\frac{3}{4}+\frac{a}{2}\right)}\right] \tag{B4}$$

and for $x >> 1$:

$$D_{-a-12}(x) \approx x^{-a-12}\mathrm{e}^{-x^2/4} \tag{B5}$$

References

Abramowitz M, Stegun IA (eds) (1972) Handbook of mathematical functions with formulas, graphs, and mathematical tables. Dover, New York

Achterhold K, Keppler C, Ostermann A, van Bürck U, Sturhahn W, Alp EE, Park FG (2002) Vibrational dynamics of myoglobin determined by the phonon-assisted Mössbauer effect. Phys Rev E 65:051 916

Berg JM, Tymoczko J, Stryer L (2002) Biochemistry, 5th edn. Freeman, New York

Branden C, Tooze J (1999) Introduction to protein structure, 2nd edn. Taylor and Francis, London

Cordone L, Ferrand M, Vitrano E, Zaccai G (1999) Harmonic behavior of trehalose-coated carbon-monoxy-myoglobin at high temperature. Biophys J 76:1043–1047

Doster W, Cusack S, Petry W (1989) Dynamical transition of myoglobin revealed by inelastic neutron scattering. Nature 337:754–756

Ferrand M, Dianoux AJ, Petry W, Zaccai G (1993) Thermal motions and function of bacteriorhodopsin in purple membranes: Effects of temperature and hydration studied by neutron scattering. Proc Natl Acad Sci USA 90:9668–9672

Frauenfelder H, McMahon B, Stojković BP (1998) Is myoglobin like a Swiss watch? In: Matsson L (ed) Proceedings of the Adriatico research conference on nonlinear co-operative phenomena in biological systems. World Scientific, Singapore, p 145

Howard J (2001) Mechanics of motor proteins and the cycloskeleton. Sinauer, Sunderland, Mass

Neinhaus GU, Heinzl J, Huenges E, Parak F (1989) Protein crystal dynamics studied by time-resolved analysis of x-ray diffuse scattering. Nature 338:665

Nienhaus GU, Waschiply R, Nienhaus K, Minkow O, Ostermann A, Parak FG (2001) Ligand migration and binding in myoglobin mutant l29w. In: Proceedings of the first biological physics conference, Bangkok, Thailand. World Scientific, Singapore, p 56

Ostermann A, Waschipky R, Parak FG, Nienhaus GU (2000) Ligand binding and conformational motions in myoglobin. Nature 404:205–208

Parak FG (2001) Fluctuations and relaxations in proteins. In: Proceedings of the first biological physics conference, Bangkok, Thailand. World Scientific, Singapore, p 7

Parak FG, Achterhold K (1999) Protein dynamics studied on myoglobin. Hyperfine Interact 123:825–840

Parak F, Knapp E, Kucheida D (1982) Protein dynamics. Mossbauer spectroscopy on deoxymyoglobin crystals. J Mol Biol 161:177–194

Steinbach PJ, Brooks BR (1993) Protein hydration elucidated by molecular dynamics simulation. Proc Natl Acad Sci USA 90:9135–9139

Steinbach PJ, Brooks BR (1996) Hydrated myoglobin's anharmonic fluctuations are not primarily due to dihedral transitions. Proc Natl Acad Sci USA 93:55–59

Tama F, Miyashita O, Kitao A, Go N (2000) Molecular dynamics simulation shows large volume fluctuations of proteins. Eur Biophys J 29:472–480

Tuszyński JA, Wierzbicki A (1991) Non-Gaussian approach to critical fluctuations in the Landau-Ginzburg model and finite-size scaling. Phys Rev B 43:8472–8481

Tuszyński JA, Clouter MJ, Kiefte H (1985) Beyond the Gaussian approximation: some new results in the Landau theory of phase transitions. Phys Lett A 108:272–276

Tuszyński JA, Clouter MJ, Kiefte H (1986) Non-Gaussian models for critical fluctuations. Phys Rev B 33:3423–3435